The Zinc Finger Protein Ynr046w Is Plurifunctional and a Component of the eRF1 Methyltransferase in Yeast

Valérie Heurgué-Hamard, Marc Graille, Nathalie Scrima, Nathalie Ulryck, Stéphanie Champ, Herman van Tilbeurgh, Richard H Buckingham

THE JOURNAL OF BIOLOGICAL CHEMISTRY VOL. 281, NO. 47, pp. 36140–36148, November 24, 2006

The Zinc Finger Protein Ynr046w Is Plurifunctional and a Component of the eRF1 Methyltransferase in Yeast*

Received for publication, September 6, 2006, and in revised form, September 28, 2006 Published, JBC Papers in Press, September 28, 2006, DOI 10.1074/jbc.M608571200

Valérie Heurgué-Hamard[‡1], Marc Graille[§1], Nathalie Scrima[‡], Nathalie Ulryck[§], Stéphanie Champ[‡2], Herman van Tilbeurgh[§3], and Richard H. Buckingham[‡4]

From the [‡]UPR 9073 du CNRS, Institut de Biologie Physico-Chimique, 13 rue Pierre et Marie Curie, 75005 Paris, France and [§]UMR8619 du CNRS, Institut de Biochimie et Biophysique Moléculaire et Cellulaire, Université Paris XI, 91405 Orsay, France

Protein release factor eRF1 in *Saccharomyces cerevisiae*, in complex with eRF3 and GTP, is methylated on a functionally crucial Gln residue by the *S*-adenosylmethionine-dependent methyltransferase Ydr140w. Here we show that eRF1 methylation, in addition to these previously characterized components, requires a 15-kDa zinc-binding protein, Ynr046w. Co-expression in *Escherichia coli* of Ynr046w and Ydr140w allows the latter to be recovered in soluble form rather than as inclusion bodies, and the two proteins co-purify on nickel-nitrilotriacetic acid chromatography when Ydr140w alone carries a His tag. The crystal structure of Ynr046w has been determined to 1.7 Å resolution. It comprises a zinc-binding domain built from both the N- and C-terminal sequences and an inserted domain, absent from bacterial and archaeal orthologs of the protein, composed of three α-helices. The active methyltransferase is the heterodimer Ydr140w·Ynr046w, but when alone, both in solution and in crystals, Ynr046w appears to be a homodimer. The Ynr046w eRF1 methyltransferase subunit is shared by the tRNA methyltransferase Trm11p and probably by two other enzymes containing a Rossman fold.

Termination codons in mRNA are recognized on the ribosome by class I protein termination factors (or release factors (RFs))[5] in eubacteria, archaea, and eukaryotes (1–3). Three codons are used as stop signals in most organisms: UAA, UGA, and UAG. In bacteria, two class I RFs are required for termination: RF1, which recognizes UAA and UAG codons, and RF2, which recognizes UAA and UGA codons. In contrast, a single RF, eRF1 or aRF1, is sufficient for termination at all three stop codons in eukaryotes and archaea, respectively. eRF1 and aRF1 form closely related protein families but are evolutionarily distinct from the eubacterial RFs (4). Thus, despite a similar function, the only sequence element common to all RFs is a tripeptide sequence, GGQ. Structural and mutational analysis shows that this motif is essential for RF activity and is required to interact with the peptidyl transferase center of the large ribosomal subunit and trigger hydrolysis of the ester bond in peptidyl-tRNA (5, 6). The Gln residue of the GGQ motif is methylated in both bacteria (7) and *Saccharomyces cerevisiae* (8, 9), and probably in mammals. Bacterial RF methylation depends on the PrmC methyltransferase (MTase) (10, 11), the product of the gene *prmC* (previously named *hemK*) situated in *Escherichia coli*, and most other bacteria immediately downstream of the gene *prfA* encoding RF1. RF methylation in *E. coli* strongly stimulates the activity of the factors (7, 11).[6]

It is remarkable that the modification of Gln in the GGQ motif is conserved from bacteria to eukaryotes despite the different evolutionary origin of the class I RFs themselves. The *S. cerevisiae* genome encodes two proteins, Ydr140w and Ynl063w, with significant similarity to bacterial PrmC that goes beyond the motifs known to be involved in AdoMet binding (7). Inactivation of *Ydr140w* was shown to lead to a loss of eRF1 methylation (8). The gene *Ynl063w* is required for methylation of the mitochondrial RF, Mrf1p (9). Methylation of eRF1 by Ydr140w differs from prokaryotic RF methylation in that the presence of the class II RF (eRF3 in yeast), and GTP was also required. The substrate of the yeast MTase therefore appears to be the ternary complex eRF1·eRF3·GTP rather than eRF1 alone. The role of class II factors in eubacteria is to catalyze the recycling of the class I RFs following peptide release (12, 13); in eukaryotic organisms the role of eRF3 seems to be closer to that of EF1α and leaves the ribosome after peptide release (14). Thus, a significant difference between eubacterial and eukaryotic factors is that, in the presence of GTP, the class I and class II factors (eRF1 and eRF3) bind to each other (15), whereas the eubacterial factors do not. Archaea appear to have no class II RF.

Some observations made during the characterization of Ydr140w as the eRF1 MTase in *S. cerevisiae* suggested that at least one further component, in addition to the ternary complex eRF1·eRF3·GTP and Ydr140w, is required for methylation of eRF1

* This work was supported by Centre National de la Recherche Scientifique Grants UPR9073 and UMR8619 and by the Génopole program and the Fondation pour la Recherche Médicale. The costs of publication of this article were defrayed in part by the payment of page charges. This article must therefore be hereby marked "*advertisement*" in accordance with 18 U.S.C. Section 1734 solely to indicate this fact.

The atomic coordinates and structure factors (code 2J6A) have been deposited in the Protein Data Bank, Research Collaboratory for Structural Bioinformatics, Rutgers University, New Brunswick, NJ (http://www.rcsb.org/).

[1] These authors contributed equally to this work.

[2] Present address: CNRS, UPR 9036, 31 chemin Joseph Aiguier, 13402 Marseille, France.

[3] To whom correspondence may be addressed: IBBMC, CNRS, UMR8619, Université Paris XI, Bât. 430, 91405 Orsay, France. Tel.: 331-6915-3155; Fax: 331-6985-3715; E-mail: herman.van-tilbeurgh@ibbmc.u-psud.fr.

[4] To whom correspondence may be addressed: IBPC, CNRS, UPR 9073, 13 rue Pierre et Marie Curie, 75005 Paris, France. Tel.: 331-5841-5120; Fax: 331-5841-5020; E-mail: richard.buckingham@ibpc.fr.

[5] The abbreviations used are: RF, release factor; AdoMet, *S*-adenosylmethionine; Ni-NTA, nickel-nitrilotriacetic acid; MTase, methyltransferase; IPTG, isopropyl β-D-thiogalactopyranoside; DTT, dithiothreitol; HIV-1, human immunodeficiency virus, type 1; GDPNP, guanine 5′-(β,γ-imido) triphosphate.

[6] L. Mora, unpublished results.

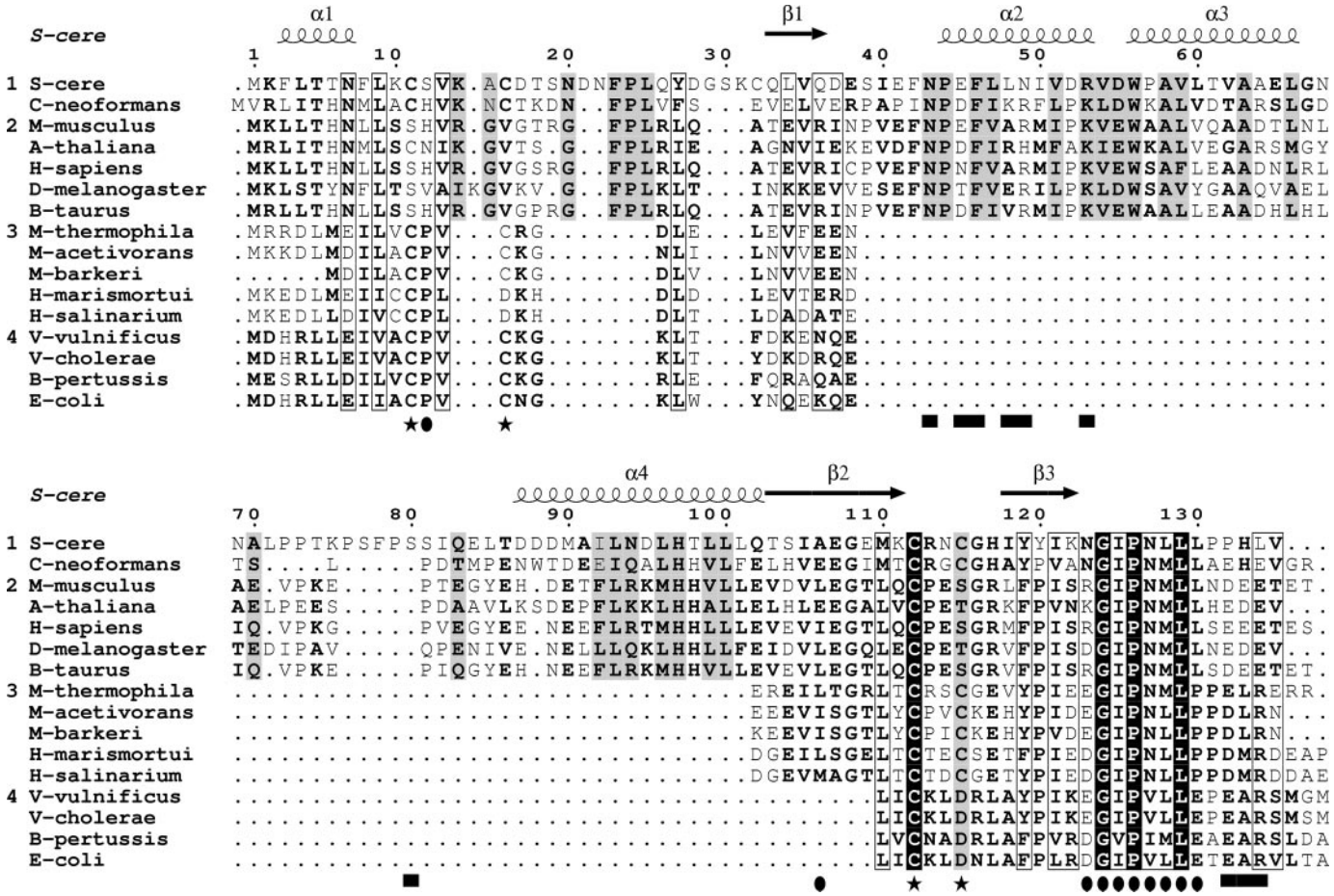

FIGURE 1. **Ynr046w sequence alignment.** *S. cerevisiae* (*S-cere*) Ynr046w secondary structure elements are superposed above the sequences. The sequences have been divided into subfamilies: fungi (*group 1*), higher eukaryotes (*group 2*), archaea (*group 3*), and eubacteria (*group 4*). Residues strictly conserved among all families are in *white* on a *black background*. Amino acids in *bold letters* and in *gray boxes* are strictly conserved within the same subfamily. Those partially conserved within the same subfamily are *boxed*. The Cys residues involved in zinc binding are indicated by *black stars* below the alignment. *Filled circles* below the alignment show residues from monomer A that contribute to homodimer formation in the crystal, whereas *filled rectangles* show those contributing from monomer B (see text).

(8). Only impure preparations of Ydr140w, produced in yeast, were able to methylate RFs *in vitro*, and with low efficiency. Overproduction of Ydr140w in *E. coli* led exclusively to insoluble protein, but even when resolubilized by routine renaturation methods, no MTase activity could be detected. Polevoda *et al.* (9) confirmed the function of Ydr140w in methylation of eRF1, but their assays were also performed with partially purified components and resulted in a low efficiency of methylation. Other studies of proteins interacting with Ydr140w in yeast, either by two-hybrid mapping or by tandem affinity purification-tagged co-purification, followed by mass spectrometry, identified Ynr046w, a 15-kDa protein, as a component interacting with Ydr140w (16, 17). Furthermore, affinity studies showed that two *S. cerevisiae* tRNA MTases, Trm11p and Trm9p, and a further protein, Lys9p, apparently bind to Ynr046w (16–18), and Purushothaman *et al.* (19) demonstrated the requirement for both Ynr046w and Trm11p for m^2G10 formation in yeast tRNA. Lys9p is a dehydrogenase with a Rossman fold similar to that in most RNA MTases. Sequence analysis has revealed the existence of Ynr046w orthologs within the three kingdoms of life (19). Interestingly, archaeal and bacterial proteins from this family are much shorter (about 55–65 residues) than eukaryotic proteins (about 130 residues; Fig. 1). Hence, Ynr046w is made of a central region specific for eukaryotic members ("insert" domain, residues 39–101) inserted within a region conserved in the three kingdoms of life ("conserved" domain, residues 1–38 and 102–135). Among fungal orthologs, this latter domain harbors a putative zinc finger signature made of the $^{11}CX_5C^{16}$ and $^{112}CX_2C^{115}$ motifs (where *X* can be any residue; from the N- and C-terminal parts, respectively).

Here we show that Ynr046w is required as a subunit of the eRF1 MTase in *S. cerevisiae*. *In vitro*, purified Ydr140w, Ynr046w, and AdoMet are necessary and sufficient to methylate the ternary complex eRF1·eRF3·GTP. Finally, we present the 1.7 Å resolution crystal structure of this small protein and show that it comprises two domains: a domain built from both N-terminal and C-terminal sequences that contains a zinc-binding site and an inserted domain, absent from bacterial and archaeal orthologs of the protein, composed of three α-helices.

EXPERIMENTAL PROCEDURES

Bacterial Growth—LB medium was supplemented according to requirements. Antibiotics were added at the following final concentration: kanamycin, 50 μg/ml; ampicillin, 200 μg/ml;

and chloramphenicol, 15 μg/ml. When induction was necessary to overexpress proteins, 1 M IPTG was added to liquid medium to a final concentration of 1 mM. For expression of Ynr046w, alone or as a complex with Ydr140w, $ZnCl_2$ was added to a final concentration of 100 μM.

Recombinant DNA Manipulations—General procedures for DNA recombinant techniques, plasmid extraction, etc. were performed as described by Sambrook *et al.* (20).

Yeast eRF1 and Truncated eRF3 Expression Vectors—pYSC1, a derivative of pET11a plasmid encoding eRF1 with a His_6 tag on its C terminus, was constructed by gene cloning between the NdeI and BamHI sites. Amplification was performed on chromosomal DNA from yeast strain yIBPC27. The upstream oligonucleotide (5′-AATACTTCACATATGGATAACGAGGT-3′) introduces an NdeI site. The downstream oligonucleotide (5′-CGCGGATCCTTTAGTGGTGGTGGTGGTGGTGAATGAAATCATAGTCGGACCCTTCA-3′) introduces a new BamHI site, eliminating the original one upstream of the stop codon, and encodes the His_6 tag. pYSC2, also a derivative of pET11a, encodes yeast eRF3 truncated at the N terminus. Amplification of genomic DNA was done with the following oligonucleotides, introducing, respectively, the NdeI site followed by the His_6 tag (5′-GGAATTCCATATGCACCACCACCACCACCACTTTGGTGGTAAAGATCACGTTTC-3′) and the BamHI site (5′-GCGGATCCTTTACTCGGCAATTTTAAC-3′).

MTase Ydr140w and Ynr046w Subunit Expression Vectors—pVH450 encodes Ynr046w with a His_6 tag at its C terminus and pVH451 encodes the same protein without tag. Both are derivatives of the pET11a vector with a kanamycin cassette and were constructed in the same way after genomic DNA amplification from yeast strain yIBPC27. The upstream oligonucleotide, 5′-TAGCCTAGTCCATATGAAGTTCTT-3′, the same in both cases, introduces an NdeI site. The downstream primers are 5′-ACACAGGGATCCCGCTTGATTTAGTGGTGGTGGTGGTGGTGTACCAGGTGTGGAGGTAACAGCAA-3′ for pVH450 and 5′-ACACAGGGATCCCGCTTGATTTATAC-3′ for pVH451.

For co-expression experiments, Ydr140w with a His_6 tag on its C terminus was also expressed from plasmid pACYCDuet (ydrH6) compatible with pET plasmids. The gene encoding Ydr140wH6 was cloned in two steps (fragment NdeI-BamHI and fragment NdeI-NdeI) between NdeI and BsrGI in the MCS2 of pACYCDuet1 (Novagen). pACYCDuet(ydrH6) was constructed from plasmid pTrc(ydr140wH6), a derivative of pVH383 itself derived from pVH371 (8). In the first step, *Ydr140w* gene was cloned from pVH371 into pLV1 between NdeI and BamHI sites to yield pVH383. A His_6 tag was then introduced by inserting phosphorylated oligonucleotides (5′-GTACAGCTTTACAAGGCACCACCACCACCACCACTGAG-3′ and 5′-GATCCTCAGTGGTGGTGGTGGTGGTGCCTTGTAAAGCT-3′) between the BsrGI and BamHI sites to give pTrc(ydr140wH6).

Protein Expression and Purification—After transformation of BL21(DE3) Rosetta by the relevant plasmids, the expression of His-tagged eRF1 or truncated His-tagged eRF3 (eRF3Ct) was induced by IPTG (1 mM) at 16 °C at an optical density (600 nm) of 0.5 in LB medium with appropriate antibiotics, followed by growth overnight. For eRF1, the cells were resuspended in buffer A1 (20 mM Tris-HCl, pH 7.5, 500 mM NaCl, 6 mM β-mercaptoethanol, and 5 mM imidazole) with EDTA-free antiprotease (Roche Applied Science) and broken by passage through a French press. After centrifugation, the supernatant was loaded on Ni-NTA resin (Sigma). The column was washed with buffer A1 and eluted with buffer A1 with 150 mM imidazole but no NaCl. Fractions containing protein were dialyzed against buffer A2 (20 mM Tris-HCl, pH 7.5, 6 mM β-mercaptoethanol) and concentrated by ultrafiltration through Amicon Ultra 30 (Millipore). For eRF3, the cells were resuspended in buffer B1 (50 mM sodium phosphate, pH 7.0, 500 mM NaCl, 6 mM β-mercaptoethanol, and 5 mM imidazole) with EDTA-free antiprotease (Roche Applied Science) and broken by passage through a French press. After centrifugation, the supernatant was loaded on Ni-NTA resin (Sigma). The column was washed with buffer B1 and eluted with buffer B1 with 150 mM imidazole but no NaCl. Fractions containing protein were concentrated by ultrafiltration through Amicon Ultra 30. Imidazole was eliminated by gel filtration on Sephadex G25 in buffer B2 (50 mM sodium phosphate buffer, pH 7.0, 6 mM β-mercaptoethanol).

Ynr046wH6 was expressed alone in BL21-Gold (DE3) (Stratagene). Co-expression of Ydr140wH6 and Ynr046w was done in the same strain at 23 °C after induction with 1 mM IPTG at an optical density (600 nm) of 0.5 in LB medium with the appropriate antibiotics, followed by growth overnight. Purification of Ynr046wH6 alone or the complex (Ydr140wH6·Ynr046) was performed as described for eRF1 purification with small modifications. Buffer A1 was modified to buffer C1 (10 mM Tris-HCl, pH 8.0, 500 mM NaCl, 6 mM β-mercaptoethanol, 10 μM $ZnCl_2$). Elution was performed with buffer C1 with 50 mM imidazole and no NaCl. Fractions containing protein were dialyzed against buffer C2 (10 mM Tris-HCl, pH 8.0, 6 mM β-mercaptoethanol, 10 μM $ZnCl_2$). Protein was concentrated by ultrafiltration through Amicon Ultra 30 for the complex and Amicon Ultra 10 for Ynr046wH6 alone.

In Vitro Recombinant Ydr140w Purification from Inclusion Bodies—Production of Ydr140w alone in *E. coli* was achieved as described by Heurgué-Hamard *et al.* (8) from pVH371. Purification was carried out according to Vuillard and Freeman (dwb.unl.edu/Teacher/NSF/C08/C08Links/www.nwfsc.noaa.gov/protocols/inclusion.html). This procedure involves solubilization of proteins from inclusion bodies by guanidinium chloride, followed by rapid dilution in the presence of nondetergent sulfobetaines to limit aggregation. The pellet from 150 ml of bacterial suspension was resuspended in 5 ml of 50 mM HEPES-NaOH, pH 7.5, 0.5 M NaCl, 1 mM phenylmethylsulfonyl fluoride, 5 mM DTT containing 0.35 mg/ml lysozyme and then incubated for 30 min at 20 °C. Triton X-100 was added to a concentration of 1% (v/v), and the cells were broken by passage through a French press. The extract was treated with DNase I (20 μg/l) for 1 h at 37 °C and centrifuged at 30,000 × *g* for 30 min at 4 °C. The pellet (inclusion bodies) was washed twice with phosphate-buffered saline containing 1% Triton X-100, centrifuged at 30,000 × *g* for 30 min at 4 °C, and then solubilized for 1 h at 4 °C in 2 ml of 50 mM HEPES-NaOH, pH 7.5, 6 M guanidine HCl, 25 mM DTT. After centrifugation at 100,000 × *g* for 10 min, the insoluble material was removed. The protein concentration in the supernatant was adjusted to 1 mg/ml (from 30 mg/ml) using 50 mM HEPES-NaOH, pH 7.5, 6 M guanidine HCl,

TABLE 1
Data collection statistics

	Native	SAD
Data collection		
Resolution (Å)	20-1.7 (1.75-1.7)	45-2.0 (2.2-2.0)
Space group	C 2	C 2
Unit cell parameters	a = 92.6 Å, b = 38.5 Å; c = 45.8 Å, β = 102.2°.	a = 92.7 Å, b = 38.5 Å; c = 45.8 Å, β = 102.2°.
Total number of reflections	42,338	57,188
Total number of unique reflections	17,182	10,322
R_{sym} (%)[a]	13.3 (52.4)	13.7 (49.2)
Completeness (%)	97.7 (99)	99.4 (99.5)
$I/s(I)$	6.2 (2.4)	9 (1.3)
Redundancy	2.5	5.5
Refinement		
Resolution (Å)	20-1.7	
R/R_{free} (%)[b]	19.8/23.6	
root mean square deviation		
Bonds (Å)	0.011	
angles (°)	1.296	
Mean B factor (Å²) protein/water	16.6/27	
Ramachandran plot		
Most favored (%)	93.3	
Allowed (%)	6.7	

[a] $R_{sym} = \Sigma_h\Sigma_i|I_{hi} - <I_h>| / \Sigma_h\Sigma_i I_{hi}$, where I_{hi} is the ith observation of the reflection h, whereas $<I_h>$ is the mean intensity of reflection h.
[b] $R_{factor} = \Sigma||F_o| - |F_c||/|F_o|$. R_{free} was calculated with a small fraction (5%) of randomly selected reflections.

25 mM DTT and then diluted 10-fold as quickly as possible with cold folding buffer (50 mM HEPES, pH 7.5, 0.2 M NaCl, 1 mM DTT, 1 M NDSB201). After 1 h at 4 °C, the protein solution was dialyzed overnight at 4 °C against 10 mM Tris-HCl, pH 7.6, 1 mM β-mercaptoethanol.

In Vitro Methylation Assays—Methylation assays were performed in buffer D (100 mM Tris-HCl, pH 7.6, 10 mM $MgCl_2$, 100 mM ammonium acetate, 2 mM DTT, 0.1 mM EDTA, 100 μg/ml bovine serum albumin) and 10 μM [^{3}H]AdoMet (0.86 Ci/mmol). GTP, GDP, or GDPNP were added at a final concentration of 1 mM. The samples were withdrawn at different times, and the reaction was stopped by cold trichloroacetic acid (5%) precipitation, followed by filtration on Whatman GF/C filters and measurement of radioactivity by scintillation counting. Each time point corresponds to 9 pmol of eRF1, 9 pmol of eRF3, and the amount of enzyme as indicated in the figure legends (3 pmol of Ydr140w and 3 pmol of Ynr046w in Fig. 4; 6 pmol of Ydr140w from inclusion bodies and 30 pmol of Ynr046wH6, purified separately, in the experiment of Fig. 3).

Western Blot Analysis—Western blot experiments were performed using rabbit anti-Ydr140w antibodies commercially prepared from pure protein produced as inclusion bodies in *E. coli*. The proteins were separated on 18% SDS-polyacrylamide gels as described by Laemmli (22). Transfer to nitrocellulose membranes and Western blotting with antibodies (diluted 5000×) were performed as described by Sambrook *et al.* (20) using a peroxidase-coupled secondary antibody (diluted 5000×), SuperSignal chemiluminescent substrate (Pierce), and Kodak X-Omat AR.

Crystallization and Resolution of the Structure—The protein was stored in 10 mM Tris-HCl, pH 8, 10 μM $ZnCl_2$, 6 mM β-mercaptoethanol. The crystals were grown at 19 °C from a 1:1 μl mixture of 10 mg/ml protein solution with 1.2 M KH_2PO_4, pH 7. For data collection, the crystals were transferred into a cryoprotectant crystallization solution with progressively higher ethylene glycol concentrations up to 30% (v/v). The 2 Å resolution single wavelength anomalous dispersion data at the zinc edge and the high resolution (1.7 Å) native data could be recorded on beamlines ID23-EH1 and ID23-EH2 (ESRF, Grenoble, France), respectively.

The structure was determined by the single wavelength anomalous dispersion method using the anomalous signal from the zinc element. The data were processed using the XDS package (23). The space group was C2 with one molecule/asymmetric unit. One zinc atom site was found with the program SHELXD in the 45–3.5-Å resolution range (24). Refinement of the zinc atom, phasing, and density modification were performed with the program SHARP (25). The quality of the final phases allowed automatic building of a partial model with the program RESOLVE (26). This model was then refined against the 1.7 Å data set with the Arp/wARP program that allowed automated construction of all the Ynr046w residues (27). This model was refined using REFMAC and rebuild with the "TURBO" molecular modeling program (afmb.cnrs-mrs.fr/rubrique113.html).

All of the residues from Met^1 to His^{136} (the first residue of the His tag) are well defined in electron density and fall within the allowed regions of the Ramachandran plot as defined by the program Procheck (28). In addition, 150 water molecules and one ethylene glycol molecule (used as cryoprotectant) have been built. Statistics for all of the data collections and refinement of the different structures are summarized in Table 1. The atomic coordinates and structure factors have been deposited into the Brookhaven Protein Data Bank under the accession number 2J6A.

RESULTS

Ynr046w/Ydr140w Interaction—Previous observations showed that Ydr140w could be efficiently overproduced in *E. coli* using the pET expression system, but only as insoluble protein present in inclusion bodies. Attempts to produce soluble protein by reducing the level of induction, growing cells at lower temperatures or co-expressing chaperones were unsuccessful. Denaturation and renaturation of protein from inclusion bodies did yield substantial amounts of soluble Ydr140w. However, the resulting protein did not have methylation activity *in vitro* and appeared to be unfolded according to circular dichroism meas-

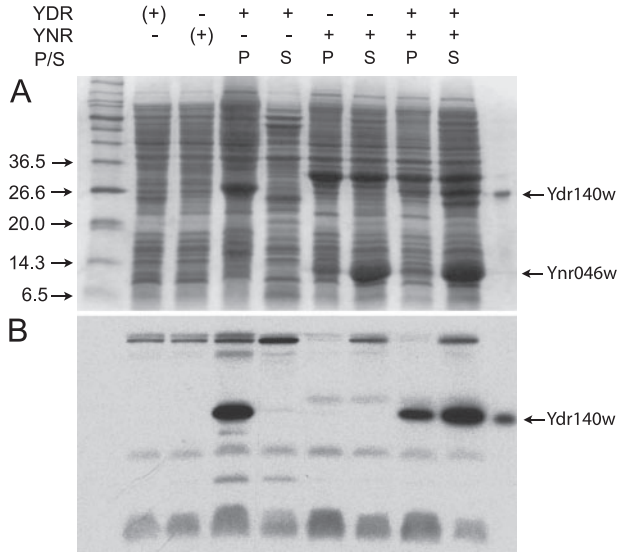

FIGURE 2. **Co-expression of Ydr140w and Ynr046w in *E. coli*.** Ydr140w and Ynr046w were overexpressed in *E. coli* strain BL21-Gold (DE3), either separately or together, with the use of compatible plasmids. The *first two lines* show the presence and absence of plasmids expressing each of the proteins; *(+)* indicates the absence of the inducer IPTG. Except for the noninduced control cultures, cell extracts were centrifuged to separate inclusion bodies (*P* indicates pellet) and soluble proteins (*S*), as indicated on the *third line*. The proteins were separated by electrophoresis in an 18% polyacrylamide-SDS gel. *A*, proteins were stained with Coomassie Blue. Molecular mass standards are shown in the *leftmost lane*, with values in kDa on the *left*, and purified Ydr140w was applied to the *lane* on the *extreme right*. *B*, a similar gel was subjected to Western blotting using polyclonal antibodies raised against purified Ydr140w.

urements.[7] On the basis of the data suggesting an interaction between Ydr140w and Ynr046w, we undertook to co-express these two proteins and study their behavior. As shown in Fig. 2, Ynr046w expressed in the absence of Ydr140w was found partly in the supernatant and partly in exclusion bodies. When expressed alone at 23 °C, Ydr140w was found exclusively in inclusion bodies, but when co-expressed with Ynr046w by the use of compatible plasmids, the major part of Ydr140w was found in the soluble fraction, together with Ynr046w (Fig. 2). An interaction between Ydr140w and Ynr046w was previously shown by TAP purification when Ynr046w was tagged (17). After co-expression in *E. coli* of His-tagged Ydr140w (Ydr140wH6) and Ynr046w, we determined whether Ynr046w could bind efficiently to Ydr140wH6 immobilized on Ni-NTA resin. The data in Fig. 3 show that the two proteins co-elute from the column at an imidazole concentration of 50 mM.

Using a similar purification protocol, Ynr046w alone did not bind to Ni-NTA resin (data not shown). Analytical gel filtration experiments realized on the Ynr046w·Ydr140wH6 purified complex shows that it has an apparent molecular mass of 46 kDa, a value slightly higher than that expected for a heterodimer (40.8 kDa, because Ynr046w and Ydr140wH6 are 15- and 25.8-kDa proteins, respectively; data not shown). In comparison, the Ynr046w protein has an apparent molecular mass of 34 kDa, a value close to that expected for a homodimer (30 kDa; data not shown).

[7] V. Heurgué-Hamard, M. Graille, N. Scrima, N. Ulryck, S. Champ, H. van Tilbeurgh, and R. H. Buckingham, unpublished data.

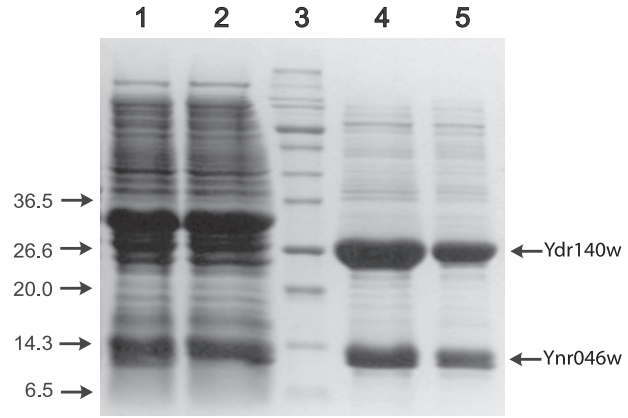

FIGURE 3. **Co-elution of His-tagged Ydr140w and nontagged Ynr046w from Ni-NTA resin with imidazole.** A cell extract from cells co-expressing the two proteins was applied to a Ni-NTA column, washed, and then eluted with buffer containing 50 mM imidazole. *Lane 1*, total protein: *lane 2*, flow-through fractions; *lane 3*, molecular mass standards (values in kDa shown on the *right*); *lanes 4* and *5*, successive fractions containing the bulk of the proteins eluted from the column with imidazole.

Ynr046w Restores Ydr140w Activity from Inclusion Bodies Purified in E. coli—The presence of physical interactions between Ydr140w and Ynr046w suggested that both proteins might be necessary for eRF1 methylation. To study this possibility, the *Ynr046w* gene, modified to encode a His_6 tag at the C-terminal part of the protein, was cloned into the expression vector pET11a. The protein was purified after overexpression in *E. coli*. *In vitro* methylation assays were performed using the ternary complex eRF1·eRF3·GTP as a substrate for the enzyme Ydr140w purified from inclusion bodies, with or without the addition of Ynr046w. As previously demonstrated, no activity is detected with Ydr140w alone. However, up to 40% eRF1 molecules are methylated when Ynr046w is added (Fig. 4), supporting the idea that Ynr046w is an essential component of the eRF1 MTase.

eRF1 Is Efficiently Methylated by the Ydr140w·Ynr046w Complex—As described above, Ydr140w and Ynr046w form a complex when co-expressed in *E. coli* and may be purified by means of a His tag on Ydr140w. *In vitro* methylation assays were performed with the complex Ydr140wH6·Ynr046w purified on Ni-NTA resin (Fig. 5). When the ternary complex eRF1·eRF3·GTP is present, 25% of eRF1 molecules are methylated within 5 min, reaching a maximum of 60% after 30 min (Fig. 5, *filled squares*). As shown previously, we confirm that eRF3 and GTP are needed for efficient modification because no methylation occurs without eRF3 and less than 5% after 60 min in presence of GDP (Fig. 5, *open circles*). The kinetics of methylation of eRF1 in the presence of eRF3 and GDPNP, a GTP nonhydrolyzable analog, show clearly that the analog can substitute for the normal nucleotide (Fig. 5, *filled triangles*). Currently available data suggest that GDPNP, a nonhydrolyzable GTP analog, does not induce a major switch in conformation of yeast eRF3 either in the case of the isolated protein (29) or when eRF3 is present with eRF1 (30). However, our data suggest that the eRF1 MTase may promote a conformational switch of the eRF3 protein to the GTP form in the presence of GDPNP.

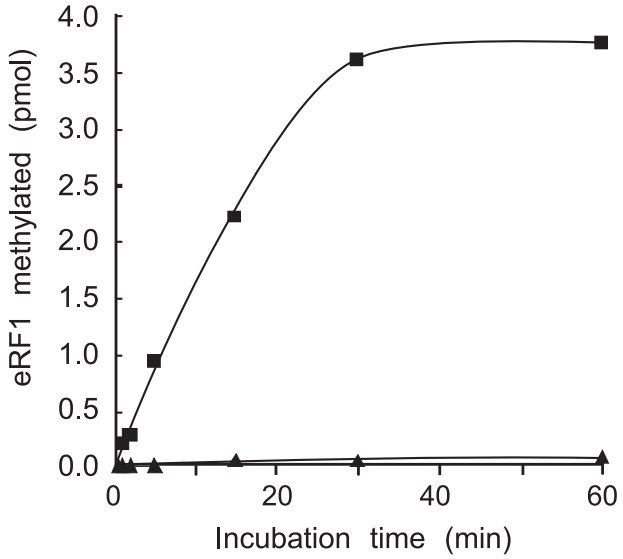

FIGURE 4. **Methylation of overexpressed yeast eRF1 by Ydr140w purified from inclusion bodies after addition of Ynr046w.** Ydr140w was overexpressed in *E. coli* and recuperated in the form of inclusion bodies. After solubilization in guanidinium chloride, the protein was renatured by rapid dilution into folding buffer (see "Experimental Procedures"). Resolubilized protein was tested for the ability to methylate eRF1, in the presence of eRF3, GTP, and [^{3}H]AdoMet, with and without addition of Ynr046w. *Filled squares*, resolubilized protein from inclusion bodies with Ynr046wH6. *Filled triangles*, resolubilized protein alone.

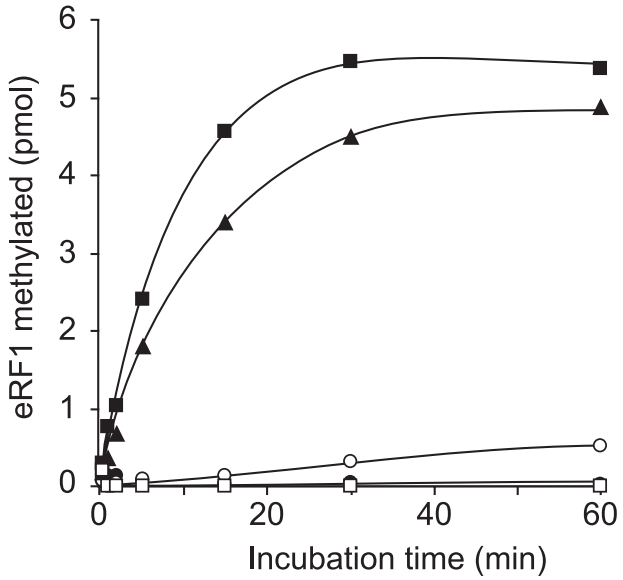

FIGURE 5. **Methylation of overexpressed yeast eRF1 by the complex Ydr140wH6·Ynr046w.** The heterodimeric enzyme complex was prepared by co-expression of the two proteins in *E. coli*, followed by purification of the complex by Ni-NTA chromatography. The complex was tested for the ability to methylate eRF1, in the presence of [^{3}H]AdoMet, with or without the addition of eRF3 and various guanine nucleotides, as follows. *Filled squares*, eRF3 and GTP; *filled triangles*, eRF3 and GDPNP; *open circles*, eRF3 and GDP; *filled circles*, eRF3; *open squares*, none.

Ynr046w Structure—Bioinformatics analysis of the Ynr046w sequence suggested the presence of a putative zinc finger region. The Ynr046w crystal structure was determined using the anomalous scattering from the zinc atom, thereby confirming zinc binding to this protein. The structure has been refined to 1.7-Å resolution, and the excellent quality of the $2F_o - F_c$ electron density map permitted the building of all of the Ynr046w residues. A single copy of Ynr046w is present in the asymmetric unit, but a homodimer can be generated by applying the crystal symmetry operators (see below). The Ynr046w monomer binds one zinc atom and has an α/β fold with approximate dimensions of $30 \times 30 \times 50$ Å^3. The conserved domain is made of a curved three-stranded anti-parallel β-sheet and the N-terminal helix α1 (Fig. 6*A*). The zinc-binding site is situated in a depression on one edge of the sheet. The helical domain is composed of three α-helices and is inserted at the opposite edge of the sheet. This insert domain packs against the helix α1 from the conserved domain.

Search for structural analogs did not provide convincing results for intact Ynr046w. However, structural homologs can be found for each domain separately. First, the zinc-binding region can be classified as a member of the "Gag knuckle" fold described by Krishna *et al.* (31). This motif is one of the 8-fold groups determined from the systematic analysis of the different zinc finger structures. However, when the zinc-binding motif of Ynr046w is compared with the prototype member of this family, the F1 zinc knuckle domain from HIV-1 nucleocapsid protein that plays a major role in the recognition and packaging of the retroviral genome (Ref. 32 and Fig. 6*B*), there is an inversion in the zinc knuckle topology. In the HIV-1 nucleocapsid protein, the two N-terminal zinc ligands come from two short strands connected by a turn (zinc knuckle) and the two C-terminal ligands from a loop. In Ynr046w, the two N-terminal zinc ligands (Cys^{11} and Cys^{16}) are located in the long loop connecting helix α1 to strand β1, whereas the two C-terminal ligands (Cys^{112} and Cys^{115}) are from the turn connecting strands β2 and β3. The α-helical insertion of Ynr046w has structural similarities to the Pit-1 POU domain, a helix bundle that recognizes defined DNA sequences (root mean square deviation of 2.9 Å over 50 of 60 Cα positions (33)). However, this is unlikely to reflect functional similarity, because the helical bundle in Ynr046w is charged negatively rather than positively, as would be expected for a DNA-binding module.

Analytical gel filtration chromatography shows that in the absence of sodium chloride, Ynr046w exists in solution as an equilibrium between a high molecular mass species (more than 200 kDa, major population) and a homodimer (34 kDa, minor population). However, when the ionic force is increased up to 0.5 M NaCl, the protein elutes exclusively as a homodimer (data not shown). The asymmetric unit of the crystal contains only one copy of the Ynr046w protein, but careful analysis of the crystal packing reveals that an asymmetric homodimer can be obtained by a crystallographic 2-fold screw axis (Fig. 6*C*). In the crystal, this homodimer is arranged so as to form parallel fibers along the crystallographic axis. This homodimer very likely corresponds to the solution dimer, and the formation of long fibers in the crystal could be driven by crystal contact forces. The homodimer buries in total 1400 Å^2 of solvent-accessible surface area, a value comparable with the average calculated for other stable protein-protein complexes (34). It has approximate dimensions of $30 \times 45 \times 65$ Å^3. Ten residues from each monomer are involved in homodimer formation (Fig. 1). Eight of ten residues from monomer A correspond to the Ynr046w peptide Asn^{123}–Leu^{130} (Fig. 1, *closed circles*), whereas residues from monomer B are mainly contributed by helix α2 from the insert

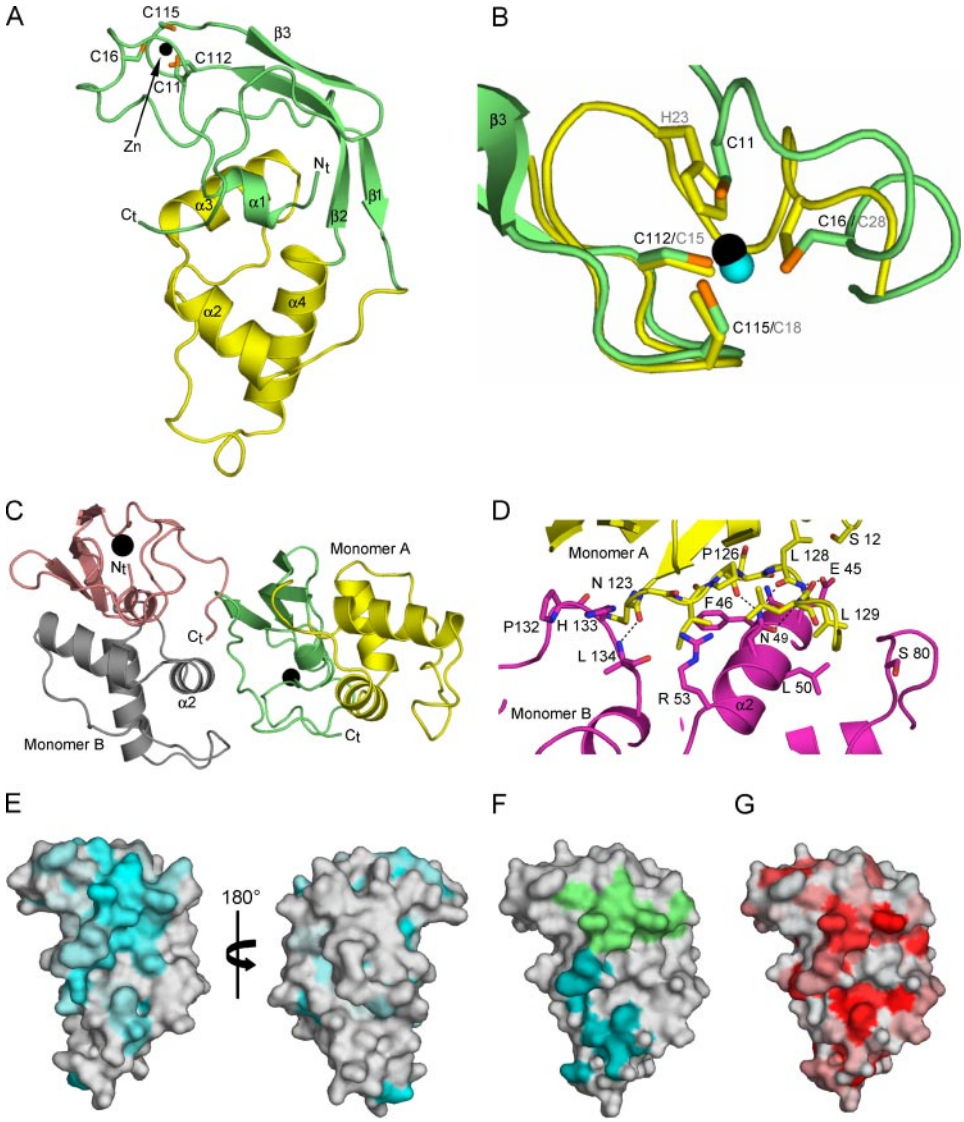

FIGURE 6. **Structure of Ynr046w.** *A*, ribbon representation of Ynr046w structure. The conserved and insert domains are colored *green* and *yellow*, respectively. The zinc atom is shown as a *black sphere*, and the Cys side chains chelating the zinc atom are shown as *sticks*. *B*, superimposition of the HIV-1 nucleocapsid protein (*yellow*, zinc atom in *blue*, and residues labeled in *gray*) on to the Ynr046w zinc finger (*green*, zinc in *black*, and residues labeled in *black*). *C*, homodimer formation in the crystal structure. *D*, close-up of Ynr046w monomer A (*yellow*) and monomer B (*magenta*) residues involved at the homodimer interface. Hydrogen bonds are depicted by *black dotted lines*. *E*, molecular surface representation of the sequence conservation among the eukaryotic Ynr046w orthologs. The *left panel* has the same orientation as in *A*, and the *right panel* is related by a 180° rotation. Coloring is from *white* (poorly conserved) to *blue* (highly conserved). *F*, surface mapping of the residues from monomers A (*green*) and B (*blue*) involved in homodimer formation. *G*, hydrophobic surface representation of the Ynr046w monomer. Polar and hydrophobic residues are colored in *white* and *red*, respectively.

domain and the C-terminal peptide Pro^{132}–Leu^{134} (Fig. 1, *closed squares*). Five hydrogen bonds are involved in homodimer formation (Fig. 6*D*). These occur between the Asn^{123} carbonyl group, the Leu^{129} and Leu^{130} amides from monomer A with the Leu^{134} amide, Glu^{45} Oϵ1 and Asn^{49} Oδ1 from monomer B, respectively. The two remaining H-bonds are between the Pro^{126} and Leu^{128} carbonyl groups from monomer A and the Asn^{49} Nδ2 atom from monomer B. In this asymmetric homodimer, the residues from monomer A involved in homodimer formation are located within the zinc-binding domain, whereas those from monomer B are mainly from the insertion as well as the C-terminal part. Because the insert domain is absent from archaeal and bacterial Ynr046w orthologs, this quaternary structure organization should be specific for the eukaryotic orthologs.

DISCUSSION

Previous work has shown that the universally conserved GGQ motif in class 1 RFs is methylated both in eubacteria and eukaryotes, and the AdoMet-dependent MTases have been identified. Here we show that yeast eRF1 methylation requires the presence of a heterodimer constituted by the MTase itself, Ydr140w, and a zinc-binding protein, Ynr046w. We have been able for the first time to reconstitute *in vitro* eRF1 methylation with purified proteins overproduced in *E. coli*. Previous *in vitro* experiments, which allowed the eRF1 MTase activity to be demonstrated, presumably depended on the fact that Ydr140w was prepared from yeast cells and that Ynr046w was present in the MTase preparation because of the affinity between the two proteins. We also confirm the need for eRF3 in its GTP conformation and show that GDPNP can substitute for GTP in the methylation reaction. Previous structural and biochemical studies of *Schizosaccharomyces pombe* eRF3, alone or in complex with GDP or GDPNP, left some doubt as to whether GDPNP was able to switch the conformation of eRF3 to the GTP form, either when present alone (29) or in complex with eRF1 (30). Our results show that the heterodimeric MTase Ydr140w·Ynr046w is able to methylate the eRF1·eRF3 complex in the presence of GTP or GDPNP but not GDP. This suggests that in the presence of the heterodimeric MTase, GDPNP is able to promote the switch of eRF3·eRF1 to the GTP conformation.

We here showed that co-expression in *E. coli* of Ynr046w and Ydr140w allows the latter to be recovered in soluble form rather than from inclusion bodies. In addition, analytical size exclusion chromatography suggests that in the presence of 0.5 M NaCl, the Ynr046w·Ydr140w complex is a heterodimer in solution, whereas Ynr046w alone forms a homodimer. This implies that binding of Ydr140w to Ynr046w hinders the formation of Ynr046w homodimer. Hence, this suggests that the Ynr046w region involved in Ydr140w binding is in close proximity or directly overlaps with the Ynr046w region involved in

homodimer formation. As shown in Fig. 6, the regions of the Ynr046w monomer involved in homodimer formation (Fig. 6*F*, *green* and *blue patches*) are very well conserved (Fig. 6*E*, blue patch) and highly hydrophobic (Fig. 6*G*, *red patch*). In addition to being responsible for homodimer formation, they are implicated in the generation of parallel fibers within the crystal. This could indicate that this region is prone to interact with other protein partners. Hence, we suspect that this particular region of Ynr046w directly interacts with Ydr140w, thereby reducing its solvent-accessible hydrophobic surface and hence reducing its tendency to aggregate. Ynr046w may also have a more active role in Ydr140w folding.

Global analyses of protein complexes in yeast (17), based on affinity data, suggest that, in addition to its interaction with Ydr140w, Ynr046w co-purifies with three other proteins: Trm11p, Trm9p, and Lys9p. Interestingly, these four proteins all share a common Rossmann-fold. Previous to this report, the interaction between Trm11p and Ynr046w has been the most extensively studied (19). Trm11p has been identified as a yeast tRNA MTase, specific for guanosine methylation. This activity is completely lost in the absence of Ynr046w, and subunit association *in vivo* has been confirmed by immunoprecipitation. However, co-expression of Trm11p and Ynr046w in *E. coli* does not seem to be sufficient to recover specific tRNA methylation activity (19). The precise function of Ynr046w in this reaction is not known, but it does not seem to play a role in Trm11p protein synthesis or life span. Ynr046w also does not directly catalyze methyl transfer on tRNA. Indeed, Trm11p possesses in principle the full functionalities to do this: a tRNA-binding site on its N-terminal domain and a MTase domain on its C-terminal domain (19).

Trm9p was identified as a novel tRNA MTase catalyzing methyl esterification of modified uridine nucleotides, resulting in the formation of mcm^5U and mcm^5s^2U (18). In this case, Trm9 fused to a glutathione *S*-transferase tag was purified in *E. coli* and shown to be active for yeast tRNA methylation. Thus, Ynr046w is not essential for the catalytic reaction, but it has not been excluded that the protein might enhance catalytic activity. Lys9p is a dehydrogenase involved in the lysine biosynthetic pathway. The enzyme was purified from yeast by Storts and Bhattacharjee (35) as a 50-kDa protein. The authors concluded that Lys9p was a monomeric enzyme, but gel filtration chromatography seemed to indicate a higher molecular mass of around 67 kDa, which would be consistent with the presence in solution of a heterodimer of Lys9p and Ynr046w. The effect of Ynr046w on the enzymatic reaction of Lys9p has not been further investigated.

The best characterized examples concerning a MTase acting with a partner concern tRNA MTases. For instance, yeast tRNA m^7G MTase Trm8p possesses AdoMet- and tRNA-binding sites and is in interaction with Trm82p. This partner seems to control the intracellular quantity of Trm8p at the protein level. The exact mechanism by which Trm82p exerts these effects is unclear. Current models propose that Trm82p possesses a chaperone-like function that protects Trm8p from degradation and/or stabilizes the MTase in an active conformation (36). Trm6·Trm61p constitutes another example of a complex involved in specific tRNA methylation. Here each partner seems to have distinct functions in catalysis; the Trm61p subunit is required for tRNA binding, whereas Trm6p binds to AdoMet and catalyzes the methylation reaction (37).

Considering the crucial role played by Ynr046w in the methylation of eRF1 and tRNA by Ydr140w and Trm11p, respectively, its precise function needs to be investigated in more detail. Orthologs of Ynr046w are widely distributed throughout the bacterial, archaeal, and eukaryotic kingdoms (19). However, the central α-helical region of the Ynr046w (residues 39–101) is found only in eukaryotic members of the extended family, whereas the N-terminal and C-terminal parts, residues 1–38 and 102–135, respectively, corresponding to the zinc finger domain, are common to all orthologs. The presence of this insert in eukaryotic proteins raises the question as to whether this domain has any specific function.

The Ynr046w zinc finger signature is located within the domain conserved in the three kingdoms of life. Sequence alignment reveals that the four Cys residues involved in zinc binding in the Ynr046w protein are strictly conserved among yeast proteins and *Methanococcales* archaea (Fig. 1). In bacteria and some archaea (*Haloarcula marismortui* and *Halobacterium salinarum*), one Cys residue is replaced by an Asp side chain (Cys^{16} for archaea and Cys^{115} for bacteria). Considering that an acidic residue is found as a zinc ligand in structural zinc sites at a frequency of 15% (38), this zinc-binding site should be conserved in bacteria and archaea. The presence of the zinc-binding site in pluricellular eukaryotes is uncertain because only Cys^{112} is conserved (Fig. 1). Cys^{11} and Cys^{115} are substituted by Ser and/or Thr, whereas Cys^{16} is replaced by Val. In Ynr046w, this zinc-binding domain has structural similarity to zinc finger regions involved in the recognition of nucleic acids (*e.g.* HIV-1 Gag nucleocapsid protein). Hence, although Trm11p possesses its own tRNA-binding site on its N-terminal domain, and Trm9p alone has been shown to be active for yeast tRNA methylation, the Ynr046w zinc finger domain could improve their affinity and specificity toward tRNA. Interestingly, a fusion of a zinc finger domain with a C-terminal MTase domain was found in another family of RNA modification enzymes, RlmAI/RlmAII, which catalyzes a specific methylation on 23 S rRNA (21). In this case, structural data showed clearly that the zinc-binding domain was involved in specific binding of the rRNA substrate. Despite the lack of structural resemblance between Ynr046w and RlmA zinc finger domains, they could have similar roles in nucleic acid binding.

In conclusion, we demonstrate that Ynr046w interacts with Ydr140w to form a stable 1:1 complex able to transfer a methyl group to the glutamine side chain of the universally conserved GGQ motif present in eukaryotic class I RFs. We show that this complex is only active on the eRF1·eRF3·GTP complex. The small Ynr046w protein (15 kDa) is built from a conserved zinc finger domain and an insert α-helical domain, the latter being present only in Ynr046w eukaryotic orthologs. Gel filtration experiments reveals that Ynr046w alone associates as a homodimer under high salt conditions, whereas it forms a heterodimer with Ydr140w. This suggests that the Ynr046w regions involved in homodimer formation and in Ydr140w formation are either overlapping or in close proximity. However, more detailed studies of complexes between Ynr046w and its

different MTases partners using a combination of structural and biochemical approaches will be required for a better understanding of its role for eRF1 methylation by Ydr140w and for tRNA methylation by Trm9p and Trm11p.

Acknowledgment—We are indebted to M. Chaillet for technical assistance.

REFERENCES

1. Kisselev, L. L., and Buckingham, R. H. (2000) *Trends Biochem. Sci.* **25,** 561–566
2. Nakamura, Y., and Ito, K. (2003) *Trends Biochem. Sci.* **28,** 99–105
3. Kisselev, L., Ehrenberg, M., and Frolova, L. (2003) *EMBO J.* **22,** 175–182
4. Kisselev, L. (2002) *Structure* (*Camb.*) **10,** 8–9
5. Petry, S., Brodersen, D. E., Murphy, F. V. t., Dunham, C. M., Selmer, M., Tarry, M. J., Kelley, A. C., and Ramakrishnan, V. (2005) *Cell* **123,** 1255–1266
6. Frolova, L. Y., Tsivkovskii, R. Y., Sivolobova, G. F., Oparina, N. Y., Serpinsky, O. I., Blinov, V. M., Tatkov, S. I., and Kisselev, L. L. (1999) *RNA* **5,** 1014–1020
7. Dinçbas-Renqvist, V., Engström, Å., Mora, L., Heurgué-Hamard, V., Buckingham, R. H., and Ehrenberg, M. (2000) *EMBO J.* **19,** 6900–6907
8. Heurgué-Hamard, V., Champ, S., Mora, L., Merkulova-Rainon, T., Kisselev, L. L., and Buckingham, R. H. (2005) *J. Biol. Chem.* **280,** 2439–2445
9. Polevoda, B., Span, L., and Sherman, F. (2006) *J. Biol. Chem.* **281,** 2562–2571
10. Graille, M., Heurgue-Hamard, V., Champ, S., Mora, L., Scrima, N., Ulryck, N., van Tilbeurgh, H., and Buckingham, R. H. (2005) *Mol. Cell* **20,** 917–927
11. Heurgué-Hamard, V., Champ, S., Engstöm, Å., Ehrenberg, M., and Buckingham, R. H. (2002) *EMBO J.* **21,** 769–778
12. Zavialov, A. V., Buckingham, R. H., and Ehrenberg, M. (2001) *Cell* **107,** 115–124
13. Freistroffer, D. V., Pavlov, M. Y., MacDougall, J., Buckingham, R. H., and Ehrenberg, M. (1997) *EMBO J.* **16,** 4126–4133
14. Alkalaeva, E. Z., Pisarev, A. V., Frolova, L. Y., Kisselev, L. L., and Pestova, T. V. (2006) *Cell* **125,** 1125–1136
15. Kobayashi, T., Funakoshi, Y., Hoshino, S., and Katada, T. (2004) *J. Biol. Chem.* **279,** 45693–45700
16. Ito, T., Chiba, T., Ozawa, R., Yoshida, M., Hattori, M., and Sakaki, Y. (2001) *Proc. Natl. Acad. Sci. U. S. A.* **98,** 4569–4574
17. Gavin, A. C., Bosche, M., Krause, R., Grandi, P., Marzioch, M., Bauer, A., Schultz, J., Rick, J. M., Michon, A. M., Cruciat, C. M., Remor, M., Hofert, C., Schelder, M., Brajenovic, M., Ruffner, H., Merino, A., Klein, K., Hudak, M., Dickson, D., Rudi, T., Gnau, V., Bauch, A., Bastuck, S., Huhse, B., Leutwein, C., Heurtier, M. A., Copley, R. R., Edelmann, A., Querfurth, E., Rybin, V., Drewes, G., Raida, M., Bouwmeester, T., Bork, P., Seraphin, B., Kuster, B., Neubauer, G., and Superti-Furga, G. (2002) *Nature* **415,** 141–147
18. Kalhor, H. R., and Clarke, S. (2003) *Mol. Cell. Biol.* **23,** 9283–9292
19. Purushothaman, S. K., Bujnicki, J. M., Grosjean, H., and Lapeyre, B. (2005) *Mol. Cell. Biol.* **25,** 4359–4370
20. Sambrook, J., Fritsch, E. F., and Maniatis, T. (1989) *Molecular Cloning: A Laboratory Manual*, Cold Spring Harbor Laboratory, Cold Spring Harbor, NY
21. Das, K., Acton, T., Chiang, Y., Shih, L., Arnold, E., and Montelione, G. T. (2004) *Proc. Natl. Acad. Sci. U. S. A.* **101,** 4041–4046
22. Laemmli, U. K. (1970) *Nature* **227,** 680–685
23. Kabsch, W. J. (1993) *J. Appl. Crystallogr.* **26,** 795–800
24. Schneider, T. R., and Sheldrick, G. M. (2002) *Acta Crystallogr. Sect. D Biol. Crystallogr.* **58,** 1772–1779
25. Bricogne, G., Vonrhein, C., Flensburg, C., Schiltz, M., and Paciorek, W. (2003) *Acta Crystallogr. Sect. D Biol. Crystallogr.* **59,** 2023–2030
26. Terwilliger, T. C., and Berendzen, J. (1999) *Acta Crystallogr. Sect. D Biol. Crystallogr.* **55,** 849–861
27. Perrakis, A., Morris, R., and Lamzin, V. S. (1999) *Nat. Struct. Biol.* **6,** 458–463
28. Laskowski, R. A., Moss, D. S., and Thornton, J. M. (1993) *J. Mol. Biol.* **231,** 1049–1067
29. Song, H., Mugnier, P., Das, A. K., Webb, H. M., Evans, D. R., Tuite, M. F., Hemmings, B. A., and Barford, D. (2000) *Cell* **100,** 311–321
30. Hauryliuk, V., Zavialov, A., Kisselev, L., and Ehrenberg, M. (2006) *Biochimie* (*Paris*) **88,** 747–757
31. Krishna, S. S., Majumdar, I., and Grishin, N. V. (2003) *Nucleic Acids Res.* **31,** 532–550
32. De Guzman, R. N., Wu, Z. R., Stalling, C. C., Pappalardo, L., Borer, P. N., and Summers, M. F. (1998) *Science* **279,** 384–388
33. Jacobson, E. M., Li, P., Leon-del-Rio, A., Rosenfeld, M. G., and Aggarwal, A. K. (1997) *Genes Dev.* **11,** 198–212
34. Lo Conte, L., Chothia, C., and Janin, J. (1999) *J. Mol. Biol.* **285,** 2177–2198
35. Storts, D. R., and Bhattacharjee, J. K. (1987) *J. Bacteriol.* **169,** 416–418
36. Alexandrov, A., Martzen, M. R., and Phizicky, E. M. (2002) *RNA* **8,** 1253–1266
37. Anderson, J., Phan, L., Cuesta, R., Carlson, B. A., Pak, M., Asano, K., Bjork, G. R., Tamame, M., and Hinnebusch, A. G. (1998) *Genes Dev.* **12,** 3650–3662
38. Alberts, I. L., Nadassy, K., and Wodak, S. J. (1998) *Protein Sci.* **7,** 1700–1716